Colloid Polym Sci (2015) 293:2147–2155
DOI 10.1007/s00396-015-3632-6

ORIGINAL CONTRIBUTION

Synthesis and structure formation of block copolymers of poly(ethylene glycol) with homopolymers and copolymers of L-glutamic acid γ-benzyl ester and L-leucine in water

David Ulkoski[1] · Annette Meister[2] · Karsten Busse[2] · Jörg Kressler[2] · Carmen Scholz[1]

Received: 2 March 2015 / Revised: 21 May 2015 / Accepted: 21 May 2015 / Published online: 3 June 2015

Abstract Block copolymers consisting of blocks of poly(amino acid)s (PAAs) derived from naturally occurring L-amino acids and biocompatibilizing poly(ethylene glycol) (PEG) are of interest for biomedical applications because of their compatibility, partial degradability, and, depending on their molecular architecture, unique self-assembly behavior. PEGylated PAAs were synthesized by α-methoxy-ω-amino PEG-initiated ring-opening polymerization, ROP, of the N-carboxyanhydrides, NCAs, of L-leucine and L-glutamic acid γ-benzyl ester. The molecular weights of the resulting di- and triblock copolymers were well controlled with narrow polydispersities, and the block copolymers were obtained in high yields (>90 %). PEGylated PAA diblock copolymers with a copolymer block of PAAs were obtained when the amino acid NCAs were polymerized as a mixture and triblock copolymers with two PAA hompolymer blocks resulted from the successive addition of the respective NCAs. Dynamic light scattering indicated that these block copolymers self-assemble when exposed to a selective solvent into micelles with hydrodynamic radii between 7 and 10 nm, which aggregate into larger structures with radii ranging between 27 and 40 nm. The coexistence and sizes of the two types of particles were corroborated by small-angle neutron scattering analyses. A detailed analysis of the micelle core structures by transmission electron microscopy suggests that the cores of the micelles do not form perfect spheres and thereby enable their continued aggregation, which is further aided by the immiscibility and subsequent phase separation of poly(L-glutamic acid γ-benzyl ester) and poly(L-leucine) blocks that constitute the PAA block.

Keywords Block copolymers · Poly(amino acid)s · Self-assembly · Light and neutron scattering

Introduction

Amphiphilic polymeric systems self-assemble into a variety of microstructures, ranging from polymeric micelles to vesicles, polymersomes, and other lyotropic phases when exposed to selective solvents [1]. Such self-assembled structures are highly important in the field of biomaterials, where explicit biological responses are expected of self-assembled delivery vehicles [2–5]. The physical and molecular factors governing polymeric self-assembly have been described in detail [6–8] using a defined packing parameter, which depends on the molecular volume and contour length of the hydrophobic segment and the interfacial area of the hydrophilic segment [9]. Hence, it becomes possible to predict which self-assembled structure an amphiphilic block copolymer will adopt based on its packaging parameter. Nevertheless, the structure formation can also be controlled by kinetic factors, especially when long polymer chains are involved [10, 11].

A multitude of chemically diverse polymeric building blocks is at our disposal, and selections are typically governed by intended applications, such as the type of delivery system

Electronic supplementary material The online version of this article (doi:10.1007/s00396-015-3632-6) contains supplementary material, which is available to authorized users.

✉ Carmen Scholz
cscholz@chemistry.uah.edu

[1] Department of Chemistry, University of Alabama in Huntsville, 301 Sparkman Drive, Huntsville, AL 35899, USA

[2] Department of Chemistry, Martin Luther University Halle-Wittenberg, 06099 Halle (Saale), Germany

and additional expected properties, as for instance, stimuli-responsiveness, biodegradability, or biostability. Poly(amino acid)s, PAAs, also referred to as polypeptides, constitute one of these polymeric building blocks that are in particular of interest to self-assembled structures for biomedical applications [12–18]. A wide spectrum of chemical and physical characteristics can be covered with PAAs as they are typically synthesized from naturally occurring L-amino acids and maintain their respective property profiles with respect to functionalities, chirality, and solubility. Unlike proteins, PAAs have no defined or specific amino acid sequence and are typically synthesized from only one or two different amino acids. When considering amphiphilic block copolymers as vehicles for the delivery of biomedically relevant substances, PAAs are exceptionally well suited because of their structural similarity to proteins. Furthermore, their L-amino acid building blocks could contribute biocompatibility since the degradation products of PAAs are again L-amino acids, which are readily absorbed by the body [19–22]. The self-assembly and packing of PAA di- and triblock copolymers were studied by Deming et al. and models illustrating the polymer interactions and subsequent self-assembly were provided. Specifically, PAAs consisting of poly(L-leucine), p(L-Leu), a hydrophobic amino acid and poly(L-lysine), p(L-Lys), an ionizable amino acid, were investigated. The formation of spherical micelles, flat membranes, curved membranes, and fibrils was discussed [23].

Poly(ethylene glycol), PEG, is a biocompatibilizing macromolecule that has found a plethora of applications [24, 25]. The stealth character that was first discovered by Abuchowski [26, 27] and that PEG lends to delivery systems [28, 29], drugs [30], and surfaces [31] sets the polymer apart from other synthetic, biomedically relevant polymers. PEG readily dissolves in water and is, because of its hydrophilicity, often used as the hydrophilic segment in amphiphilic block copolymers used in drug delivery [32]. Block copolymers of PEG and PAAs are readily synthesizable, e.g., by using end-group functionalized PEG as macroinitiator in the ring-opening polymerization, ROP, of *N*-carboxyanhydrides, NCAs, of amino acids [33–36]. These amphiphilic block copolymers have been designed primarily for drug delivery [14] and gene delivery [37]; here, typically one of the amino acid building blocks is the cationic p(L-Lys) and surface modifications [33, 38–41]. For drug and gene delivery purposes, the molecular weights of block copolymers are kept low to allow for ready clearance from the system; however, the synthetic method allows for the synthesis of high molecular weight PAAs as well [33]. The microstructure of these self-assembled constructs is of importance as it has an impact on several biological key parameters of the delivery system. Various techniques exist to characterize the morphology and size of self-assembled structures directly in the selective solvent, which for biomedical applications is usually water. These methods include dynamic light scattering, DLS, cryogenic transmission electron microscopy, cryo-TEM, and sub-resolution limit fluorescence microscopy [42]. Moreover, the size of dissolved molecules and their aggregates, e.g., micelles and vesicles, can be determined by small-angle neutron scattering, SANS. In contrast to X-ray scattering measurements, the hydrophilic PEG components dissolved in water can also be detected in neutron scattering experiments by simply varying the H_2O to D_2O ratio, thus matching the respective scattering lengths [43]. This manuscript describes the synthesis of PEGylated PAAs with the PAA block consisting of poly(L-glutamic acid γ-benzyl ester), p(Bz-L-Glu), and p(L-Leu) whereat the two PAAs form either two homopolymer blocks or one copolymer block. The hydrophobic p(L-Leu) block is unreactive and will drive self-assembly in an aqueous system. Moreover, an additional structural variability is introduced with the p(Bz-L-Glu) segment: the block is highly hydrophobic, i.e., inducing self-assembly, when the terminal carboxyl groups of the side chains are protected as benzyl esters and can turn hydrophilic after deprotection to p(L-Glu). In its deprotected form, p(L-Glu) is reactive and could covalently or electrostatically bind to biomedically active substances to be delivered by these microstructures. The size of the self-assembled structures was determined by DLS and SANS, and results were corroborated by TEM measurements. These amphiphilic block copolymers self-assemble, and independent of their molecular architecture, a bimodal distribution of block copolymer aggregates was observed.

Experimental section

Materials

All chemicals were obtained from Sigma-Aldrich Chemicals Co., St. Louis, MO, and used as received, unless stated otherwise. The macroinitiator α-methoxy-ω-amino poly(ethylene glycol), $mPEG_{114}$-NH_2 (M_w=5000 g mol^{-1}) was purchased from Laysan Bio, Arab, AL. The amino acids γ-benzyl-L-glutamate (Bz-L-Glu) and L-leucine (L-Leu) were purchased from Bachem, Torrence, CA. Triphosgene was purchased from Tokyo Chemical Industry Co., Ltd., Japan, and (1S)-(−)-alpha-pinene from Fisher Scientific, Waltham, MA. These reagents were stored in a refrigerator. Deuterium oxide (D_2O) 99.9 % was obtained from Cambridge Isotope Laboratories, Inc. Dimethylformamide (DMF) was distilled over CaH_2 under vacuum. Water was deionized with a Millipore Milli-Q system.

Instrumentation

^{1}H NMR spectra were recorded on a Varian Unity Inova 500 (500 MHz) spectrometer equipped with a 5-mm triple resonance inverse detectable probe. DMSO-d_6 and trifluoroacetic

acid-d were used as solvents. All spectra were recorded at 25 °C.

Dynamic light scattering analyses were conducted using 90Plus Particle Size Analyzer (Brookhaven Instruments) at λ=532 nm and a scattering angle of 90°, a single-angle approach is sufficient for the polymer studied here. All measurements were analyzed by BIC software (Brookhaven Instruments), and diameter results are obtained from the mean radius of lognormal size distribution. Sample preparation: block copolymers (10 mg) were dissolved in 3 mL of tetrahydrofuran (THF). The organic phase was added dropwise into the aqueous phase (10 mL) and gently stirred at 35–40 °C in a warm oil bath until the evaporation of the organic solvent was complete (at least 12 h). If necessary, adequate amounts of DI water were added to obtain a 1.0 mg/mL stock concentration. The aqueous solution was filtered (0.45-μm Millex micropore Millipore poly(vinylidene fluoride), PVDF, filter) directly into a dust-free sample cell, and five measurements were carried out.

Small-angle neutron scattering, SANS, measurements were performed at the BL-6B (EQ-SANS), Spallation Neutron Source, at Oakridge National Laboratory, ORNL, using a 4-m sample to detector distance, 60-Hz operation mode, and two neutron wavelength bands with minima of 2.5 and 9.5 Å. Samples were prepared following the same protocol described above for DLS studies and loaded into 1 mm path length quartz cells. Standard corrections for background, detector efficiency, and intensity calibrations were performed. Pure D_2O was used as solvent; sample concentration was between 1.7 and 1.8 wt.%. All measurements were performed at 20 °C.

Gel permeation chromatography, GPC, analyses were conducted using an Agilent 1200 system (Gastorr GT-14 degasser, Agilent 1200 series isocratic pump and auto sampler) equipped with three Phenomenex 5 μm, 300×7.8 mm columns [100, 1000 Å, and linear] and two detectors: a Wyatt DAWN EOS multi-angle light scattering, MALS, detector (GaAs 30-mW laser at 690 nm) and a Wyatt Optilab rEX differential refractive index, DRI, detector with a 690 nm light source. DMF with 0.1 M LiBr was used as eluent at a flow rate of 0.5 mL/min. Wyatt Astra 6.0 software was used to process all SEC data. Polystyrene standards were used for the calibration. Sample preparation: block copolymers were dissolved in DMF/LiBr (0.01 M) at a concentration of 5 mg/mL and filtered (0.25 μm poly(tetrafluoro ethylene), PTFE, syringe filter).

Transmission electron microscopy was performed using an EM 900 transmission electron microscope (Carl Zeiss, Oberkochen, Germany). Micrographs were taken with a SSCCD SM-1k-120 camera (TRS, Moorenweis, Germany). Sample preparation: an aqueous polymer suspension (1 mg/mL), 5 μL, was spread onto a carbon-coated Cu grid (PLANO, Wetzlar, Germany). After 1 min, excess liquid was blotted with filter paper, and the grids were exposed to freshly prepared RuO_4 via the gas phase for 10 or 20 min, and the dried specimens were examined.

Polymer syntheses

Synthesis of L-glutamic acid γ-benzyl ester *N*-carboxyanhydride, Bz-L-Glu-NCA. NCAs of Bz-L-Glu were synthesized in dry ethyl acetate, EthAc. In a typical reaction, Bz-L-Glu (2.0 g, 8.43 mmol), pre-dissolved triphosgene (2.752 g, 9.273 mmol), and α-pinene (2.41 g, 17.7 mmol) were dissolved in 40 mL EthAc, all under open atmosphere. (Note: Triphosgene is kept at 0 °C prior to weighing it.) The reaction mixture was heated to reflux (105 °C) under stirring until the mixture became transparent. Glassware and stir bars were dried at 145–155 °C for 24 h. Gas evolution was routed through the top of the condenser into a potassium hydroxide, KOH, bubbler. The mixture was cooled and filtered; the filtrate was concentrated via rotary evaporation under reduced pressure. Crystallization was performed within a mixture of EthAc/hexane using a standard freezer at −20 °C. The crystals were filtered, vacuum dried, and redissolved in a minimal amount of EthAc at 25 °C. Sufficient amounts of hexane were added until cloudiness persisted. The suspension was filtered into a Schlenk flask purged with dry argon gas, put into an ice bath, and hexane was added until recrystallization occurred. The crystals were filtered, vacuum-dried, and characterized by ^{1}H NMR: (DMSO-d_6, 500 MHz): δ/ppm=1.94–2.05 (m, 2H, –CH_2–CH_2–CH–), 2.47 (m, 2H, –CH_2–CO–), 4.45–4.58 (t, 1H, –CO–CH–NH–), 5.10 (m, 2H, C_6H_5–CH_2–), 7.36 (m, 5H, C_6H_5–), 9.04 (br, 1H, –CO–NH–CH–); yield 85–90 %.

Synthesis of L-Leucine *N*-Carboxyanhydride, Leu-NCA. L-Leu NCA was synthesized in dry EthAc. L-Leu (1.0 g, 7.624 mmol), triphosgene (2.715 g, 9.15 mmol), and α-pinene (2.177 g, 16.01 mmol) were dissolved in 40 mL EthAc. The synthesis, isolation, and purification of the L-Leu NCA followed the same procedure described above for the Bz-L-Glu NCA. L-Leu NCA was characterized by ^{1}H NMR: (DMSO-d_6, 500 MHz): δ/ppm=0.87–0.90 (m, 6H, $(CH_3)_2$–), 1.55–1.58 (m, 2H, –CH_2–CH–$(CH_3)_2$), 1.73–1.74 (m, 1H, –CH–$(CH_3)_2$), 4.43–4.46 (m, 1H, –CO–CH–NH–), 9.07 (br, 1H, –CO–NH–CH–); yield 85–90 %.

Synthesis of methoxy-poly(ethylene glycol)-*b*-poly(L-glutamic acid γ-benzyl ester)$_x$-*b*-poly(L-leucine)$_y$, mPEG$_{114}$-*b*-p(Bz-L-Glu)$_x$-*b*-p(L-Leu)$_y$, methoxy-poly(ethylene glycol)-*b*-poly(L-leucine)$_y$-*b*-poly(L-glutamic acid γ-benzyl ester)$_x$, mPEG$_{114}$-*b*-p(L-Leu)$_y$-b-p(Bz-L-Glu)$_x$, and methoxy-poly(-ethylene glycol)-*b*-poly((L-glutamic acid γ-benzyl ester)$_x$-*co*-(L-leucine)$_y$), mPEG$_{114}$-*b*-p((Bz-L-Glu)$_x$-*co*-p(L-Leu)$_y$). Glassware and stir bars were dried at 145–155 °C for 24 h, and all materials were vacuum dried for 12 h. A typical ROP is described here for the triblock copolymer mPEG$_{114}$-*b*-p(Bz-L-Glu)$_{20}$-*b*-p(L-Leu)$_{10}$. All other polymers were synthesized by the same method using respective NCA monomer feed ratios; mPEG$_{114}$-NH_2 was used as macroinitiator in all ROPs. Urea (75.39 mg, 1.26 mmol) was dissolved in 6.3 mL of DMF under argon and degassed under vacuum. Using a dry syringe

and needle, 2 mL of the urea/DMF mixture was extracted and added to dissolve $mPEG_{114}$-NH_2 (340.9 mg, 0.0628 mmol) under argon. Light warming with a heat gun aids in fully dissolving the macroinitiator. The $mPEG_{114}$-NH_2/urea/DMF mixture was degassed for an additional 5 min. The remainder of urea/DMF mixture was used to dissolve the Bz-*L*-Glu NCA (333 mg, 1.26 mmol) under argon. The $mPEG_{114}$-NH_2/urea/DMF mixture was quickly added via syringe to the Bz-*L*-Glu NCA to initiate the reaction under argon. The polymerization was conducted for 1–2 days, while periodically purging the sample of CO_2 and replacing with argon. The reaction is complete when the gas evolution and, hence, buildup of pressure ceased. *L*-Leu-NCA (100 mg, 0.63 mmol) was added to the reaction flask under argon. The polymerization was conducted for several more days until the gas evolution stopped, indicating that the monomer was completely consumed. Reaction times depend on PAA chain lengths and typically ranged between 1 and 2 days per block. The reaction mixture was concentrated by rotary evaporation. THF was added to the crude product and stirred for 30 min. The solution was then filtered in order to remove urea. The filtrate was concentrated again to 1–2 mL of solution and placed into a dialysis bag. The polymer was purified by dialysis against distilled water for 2 days using a Spectra/Por CE membrane (MWCO 3500 g/mol) and isolated by freeze-drying. The polymer was characterized by ^{1}H NMR: (TFA-d, 500 MHz): δ/ppm=1.06–1.12 (m, 6H, $(CH_3)_2$–), 1.77–1.78 (br, 2H, –CH_2–CH–$(CH_3)_2$), 1.81–1.89 (br, 1H, –CH–$(CH_3)_2$), 2.13–2.35 (m, 2 H, –CH_2–CH_2–CO–), 2.63–2.77 (m, 2H, –CH_2–CO–), 3.72 (s, 3H, CH_3–O–), 4.05 (s, 4H, –O–CH_2–CH_2–), 4.83–4.86 (t, 2H, –CO–CH–NH–), 5.24–5.37 (m, 2H, C_6H_5–CH_2–), 7.38–7.47 (m, 5H, C_6H_5–); yields 89–95 %.

Results and discussion

Polymer synthesis

NCAs used throughout this work were produced following the Fuchs-Farthing method [44] and were polymerized by ROP under anhydrous conditions at room temperature [45]; the general reaction scheme is provided in Scheme 1. Depending on the PAA block length, reaction times ranged between 24 and 48 h per block with a total reaction time of 72–96 h and with the triblock copolymers with a total of 40 amino acid units taking the longer times. The polymerization method used here is similar to that described by Wooley [46], but polymerizations were performed under an argon blanket, in the presence of urea, and the progress of the ROPs was monitored via the CO_2 development. Reactions were considered complete when no more CO_2 was released from the reaction mixtures. As shown in Table 1, the block length of the respective PAA blocks matches closely the monomer feed ratios of Bz-*L*-Glu NCA: *L*-Leu NCA=20:10 (samples 1, 3, and 5) or 20:20 (samples 2, 4, and 6), respectively. Degrees of polymerizations and molecular weights were calculated from ^{1}H NMR data by comparing the integrals of the backbone methine groups (chiral carbons) of the PAA blocks at 4.8 ppm with the protons of the terminal methoxy group of PEG, 3.6 ppm, and the main PEG signal at 3.4 ppm; the results were further verified using the proton signals of the benzyl ester *L*-Glu protective group with the phenyl ring protons at 7.4 ppm and protons of the benzyl methylene proton at 5.2–5.3 ppm. A representative ^{1}H NMR spectrum of $mPEG_{114}$-*b*-$p(Bz\text{-}L\text{-}Glu)_{20}$-*b*-$p(L\text{-}Leu)_{10}$ is shown in the Supplemental Information, Figure SI 1.

Our previous research has shown that amino-terminated PEG with a molecular weight of 5000 g mol^{-1} (degree of polymerization of 114) is a suitable macroinitiator for NCA ROP yielding PEGylated PAA di- and triblock copolymers [33–36]. Diblock copolymers, PEG-*b*-$p((Bz\text{-}L\text{-}Glu)_x$-*co*-$(L\text{-}Leu)_y)$, form when the NCAs of benzyl-*L*-glutamate and *L*-leucine are added as a mixture, triblock copolymers form when the two respective NCAs are added successively. The formation of PEGylated PAA triblock copolymers is readily possible as the chain ends of the respective PAA blocks remain living after the first NCA monomer is consumed. The ROP of amino acids is typically characterized by low polydispersities [47], and the results obtained by GPC show PDI values for triblock copolymers range between 1.04 and 1.09. If the NCAs of Bz-*L*-Glu and *L*-Leu are added as a mixture, yielding a PAA copolymer and an overall diblock copolymer, the PDIs are slightly higher ranging between 1.10 and 1.15. These higher polydispersities have been observed before for PAA copolymers [34] and are attributed to differences in the reactivity of the two amino acid NCAs.

Previous research has also shown that the formation of secondary structures (β-sheets) in the early stages of the polymerization interferes with chain growth leading to broad molecular weight distributions. Hence, ROPs were conducted in the presence of 0.2 M urea, which efficiently suppresses the hydrogen bond formation between nascent chains, the cause for the formation of these secondary structures [48]. The molecular architecture of the resulting block copolymers can be further controlled, as the p(Bz-*L*-Glu) block can form the central, $mPEG_{114}$-*b*-$p(Bz\text{-}L\text{-}Glu)_x$-*b*-$p(L\text{-}Leu)_y$, as well as the terminal block, $mPEG_{114}$-*b*-$p(L\text{-}Leu)_y$-*b*-$p(Bz\text{-}L\text{-}Glu)_x$. The p(Bz-*L*-Glu) block is highly hydrophobic when protected as a benzyl ester.

Dynamic light scattering and small-angle neutron scattering measurements

DLS measurements on 1 wt.% polymer solutions in H_2O show a clear bimodal distribution of particles for all samples independent of block length and molecular architecture

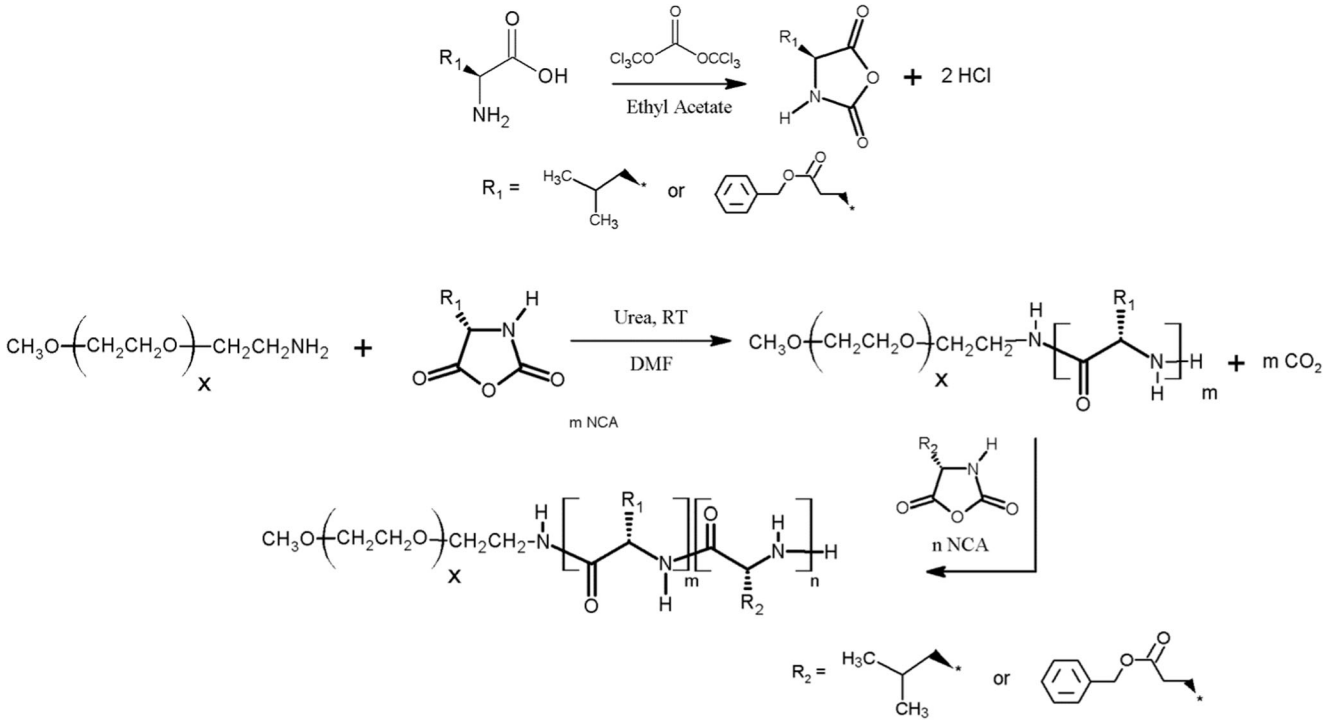

Scheme 1 Synthesis of PEGylated PAAs using a monofunctional α-methoxy-ω-amino PEG with a molecular weight of 5000 g mol^{-1} as macroinitiator. Amino acid NCAs were synthesized from the respective amino acid and triphosgene. The amino acid NCAs were added successively yielding an mPEG$_{114}$-*b*-PAA1-*b*-PAA2 triblock copolymer (samples 1, 2, 3, and 4) or as a mixture yielding mPEG$_{114}$-*b*-PAA1-*co*-PAA2 diblock copolymer (samples 5 and 6)

(Table 2). A typical DLS spectrum is shown for mPEG$_{114}$-*b*-p(Bz-*L*-Glu)$_{20}$-*b*-p(*L*-Leu)$_{10}$ in Fig. 1. Graphs for all other samples can be found in the Supplementary Information (Figure SI 2). Overlaying the DLS data with the results of SANS, Fig. 1, shows that the maxima of the DLS particle size distribution (hydrodynamic radius R_H) are in good agreement with the SANS data (radius of gyration R_G). A representative analysis is shown in Fig. 1. The radius of gyration is obtained from SANS scattering intensity I by $I = \sum a_i e^{-R_{Gi}^2 q^{2/3}}$ for three species (i=1–3) after background correction with the intensities a_i and the scattering vector $q = \frac{4\pi}{\lambda}\sin\theta$. The fit of the SANS data assuming three entities is shown in Fig. 2 for sample mPEG$_{114}$-*b*-p(Bz-*L*-Glu)$_{20}$-*b*-p(*L*-Leu)$_{10}$, all other fitting curves are shown in the Supplementary information (Figure SI 3).

The dimensions of the structures should be compared with characteristic dimensions of the molecules. For amino acids, a contour length of unfolded structures can be estimated with ~3.8 Å per monomer unit [49]. This number agrees with the persistence length of PEG or approximately one monomer unit of PEG [50, 51]. For a rough estimation of the size of a single-block copolymer chain in water, the results of neat PEG from Devanand and Selser [52] for R_G=1.95 $n^{0.583}$ Å and R_H= 1.26 $n^{0.571}$ Å are used with the degree of polymerization n. The R_G values of 3.5–3.8 nm measured for our polymers consisting of 144 to 163 monomer units (PEG and PAA) are in agreement with R_{G1} values from SANS measurements. The

Table 1 List of block copolymers synthesized, their composition, and chemical characteristics. The macroinitiator α-methoxy-ω-amino poly(ethylene glycol), mPEG$_{114}$-NH$_2$, with a molecular weight of M_w=5000 g mol^{-1} was used in the synthesis of all block copolymers

Sample	Polymer composition	Molecular weight, M_n, by NMR [g mol^{-1}]	PDI by GPC
1	mPEG$_{114}$-*b*-p((Bz-*L*-Glu)$_{20}$-*b*-p(*L*-Leu)$_{10}$)	10,500	1.04
2	mPEG$_{114}$-*b*-p((Bz-*L*-Glu)$_{24}$-*b*-p(*L*-Leu)$_{23}$)	12,900	1.06
3	mPEG$_{114}$-*b*-p((*L*-Leu)$_{12}$-*b*-p(Bz-*L*-Glu)$_{22}$)	11,200	1.05
4	mPEG$_{114}$-*b*-p((*L*-Leu)$_{23}$-*b*-p(Bz-*L*-Glu)$_{24}$)	12,800	1.09
5	mPEG$_{114}$-*b*-p((*L*-Leu)$_{12}$-*co*-(Bz-*L*-Glu)$_{23}$)	11,400	1.11
6	mPEG$_{114}$-*b*-p((*L*-Leu)$_{23}$-*co*-(Bz-*L*-Glu)$_{26}$)	13,300	1.15

Table 2 Hydrodynamic radii and radii of gyration for PEGylated PAAs

Sample	$R_{H,1}$ [nm]	$R_{H,2}$ [nm]	$R_{G,1}$ [nm]	$R_{G,2}$ [nm]	$R_{G,3}$ [nm]
1	7.3	33.3	3.0	9.3	32.4
2	9.2	40.2	3.2	9.5	41.2
3	9.2	32.9	3.9	8.6	38.5
4	12.0	35.6	4.5	10.2	27.4
5	10.2	30.6	4.8	12.9	33.8
6	8.7	26.8	4.9	11.7	25.3

corresponding R_H signals at around 2.2 nm have not been observed by DLS, which may have two reasons: in DLS measurements, the signal intensity of single chains is strongly suppressed, when larger particles are observed at the same time, and therefore, the signal of single molecules is too weak to be detected. On the other hand, it should be kept in mind that DLS measures particle sizes based on diffusion and therefore detects only free particles, whereas SANS also observes inner structures of aggregates [53], which could be either a single chain or the core of a small micelle, formed by the PAA part of several polymer chains (i.e., about five molecules in case of a flexible structure or less for stiff PAA blocks).

Amphiphilic PEGylated PAAs solutions in H_2O show a bimodal distribution in DLS upon exposure to the selective solvent water, with two distinct effective hydrodynamic radii R_H; one ranging at a size that is characteristic for polymeric micelles ($R_{H,1}$ ~7 to 10 nm), and the other one is indicative of agglomerates ($R_{H,2}$ ~26 to 40 nm). The radius of gyration, R_G, obtained from SANS measurements in D_2O, gives also an indication for even smaller structures ($R_{G,1}$ ~3 to 5 nm), which can be identified as single molecules.

Assuming a micellar structure with a core formed by a larger number of amino acids and a shell of PEG, the maximum core radius can be estimated from the PAA contour length, i.e., 30×0.38 nm=11.4 nm for sample 1 or 49×0.38 nm=18.6 nm for sample 6. The thickness of the PEG shell should be of the order of two R_H of a single PEG chain, 1.9 nm, assuming a similar equilibrium formation of the PEG chain in water. Of course, copolymers with a more hydrophobic part than the PAAs used here have a higher tendency for core formation which results in a stress on the PEG block leading to more extended structures and therefore thicker shells. Nevertheless, the observed radii of 7–10 nm ($R_{H,1}$ from DLS and $R_{G,2}$ from SANS, Table 2) are in good agreement with the expected dimension of a micelle. The larger structures of 26–40 nm ($R_{H,2}$ from DLS and $R_{G,3}$ from SANS, Table 2) cannot be explained by a simple micellar shape, i.e., micelles interact to form aggregates, see Scheme 2.

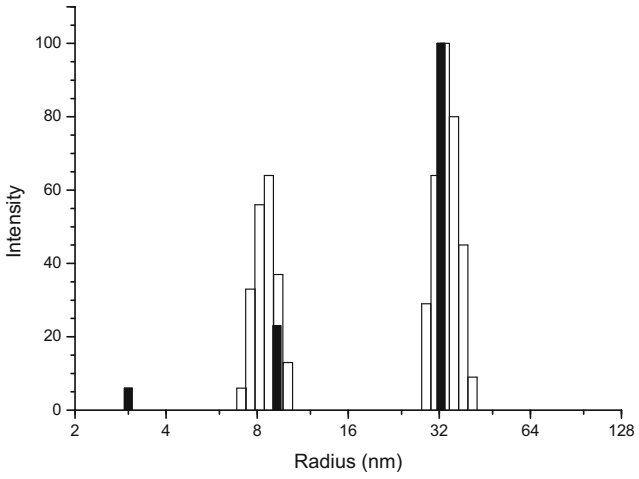

Fig. 1 Apparent hydrodynamic radius (R_H) distribution from DLS analysis (*open bars*) and radius of gyration (R_G) from SANS analysis (*black bars*) with their relative intensities for $mPEG_{114}$-*b*-p(Bz-*L*-Glu)$_{20}$-*b*-p(*L*-Leu)$_{10}$ (sample 1)

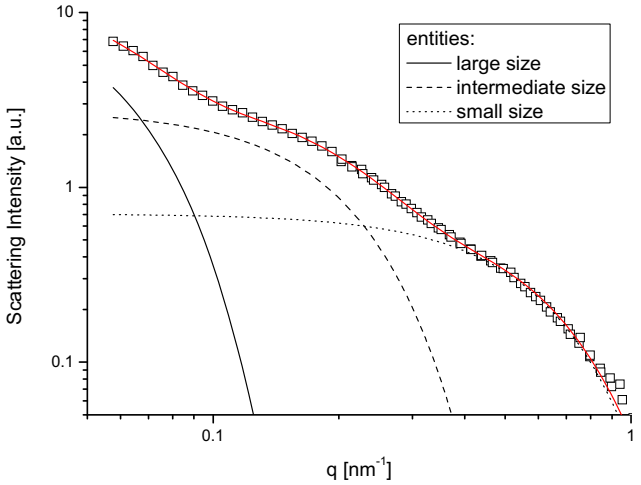

Fig. 2 SANS fit for sample 1 (*red curve*) with entities of large, intermediate, and small size. The sum of all three components is also shown in the graph

Transmission electron microscopy analyses

The negative stain TEM image of sample 1 ($mPEG_{114}$-*b*-p(Bz-*L*-Glu)$_{20}$-*b*-p(*L*-Leu)$_{10}$) that is shown in Fig. 3 is representative for the PEGylated PAA block copolymers investigated here and is very similar to the images published by Gu et al. [54] for their PEG-*b*-poly(racemic leucine) diblock copolymers. The sample was cast onto a carbon grid from an aqueous solution and dried at room temperature. Then, the sample was subjected to a ruthenium tetroxide, RuO_4, vapor phase, which preferentially stains the aromatic rings of the benzyl-protected p(Bz-*L*-Glu) blocks [55]. Conducting TEM analyses on the deprotected block copolymer yields no contrast, and no polymeric structures can be observed (see inset of Fig. 3a). The image a in Fig. 3 shows micelles and larger aggregates with similar dimension as observed for the two populations by DLS in water. Of course, only the core of the micelles is observed, the hydrophilic PEG corona does not provide any contrast for TEM. The large aggregates are also

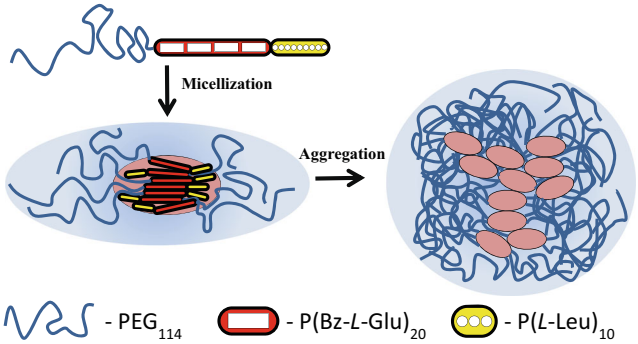

Scheme 2 Graphical depiction of the formation of polymeric aggregates: single chains form micelles, which then aggregate into larger structures

heterogeneous so that the formation of polymersomes can be excluded. It appears that aggregates of micelles are formed. It is reasonable to assume that the micelle core has similar dimensions in the dried TEM sample and in water since the core is formed by strongly hydrophobic blocks [56]. Nevertheless, it is necessary to state that the dimensions of micelles and aggregates obtained by scattering methods and by TEM might differ significantly due to strong influences of the evaporation conditions of the solvent. The image b provides a higher magnification, indicating already that the cores of the micelles do not form perfect spheres. Possible intermediate structures of the aggregation process are depicted for characteristic examples in image c of Fig. 3. The larger aggregates show how micelles add themselves onto existing polymer aggregates. Both the p(Bz-*L*-Glu)$_{20}$ and p(*L*-Leu)$_{10}$ blocks are very hydrophobic and exist as stiff molecules in an aqueous environment. Furthermore, these blocks are not miscible with each other, which leads to a phase separated micelle core. This can be seen in the image d, where the sample was stained with RuO_4 vapor for only 10 min as opposed to the 20 min exposure used for all other samples. Because RuO_4 stains preferably aromatic rings, it can be assumed that the dark entities are formed by the p(Bz-*L*-Glu)$_{20}$ block. It is clearly visible that the stained fractions of the core are not spherical. This irregularity may lead to an inhomogeneous distribution of the PEG corona around the micelle core, see Scheme 2. Thus, in aqueous solution, the micelle cores are not completely shielded by giving rise to micelle core contacts and finally to the fusion of micelles into large inhomogeneous aggregates seen in the TEM images.

Conclusions

Di- and triblock copolymers of PEG and p(Bz-*L*-Glu), p(*L*-Leu), and p(Bz-*L*-Glu-*co*-*L*-Leu) have been prepared successfully by ROPs of the NCAs of the respective amino acids with mPEG$_{114}$-NH$_2$ serving as the macroinitiator. The molecular weight of the PAA blocks was tightly controlled and matched

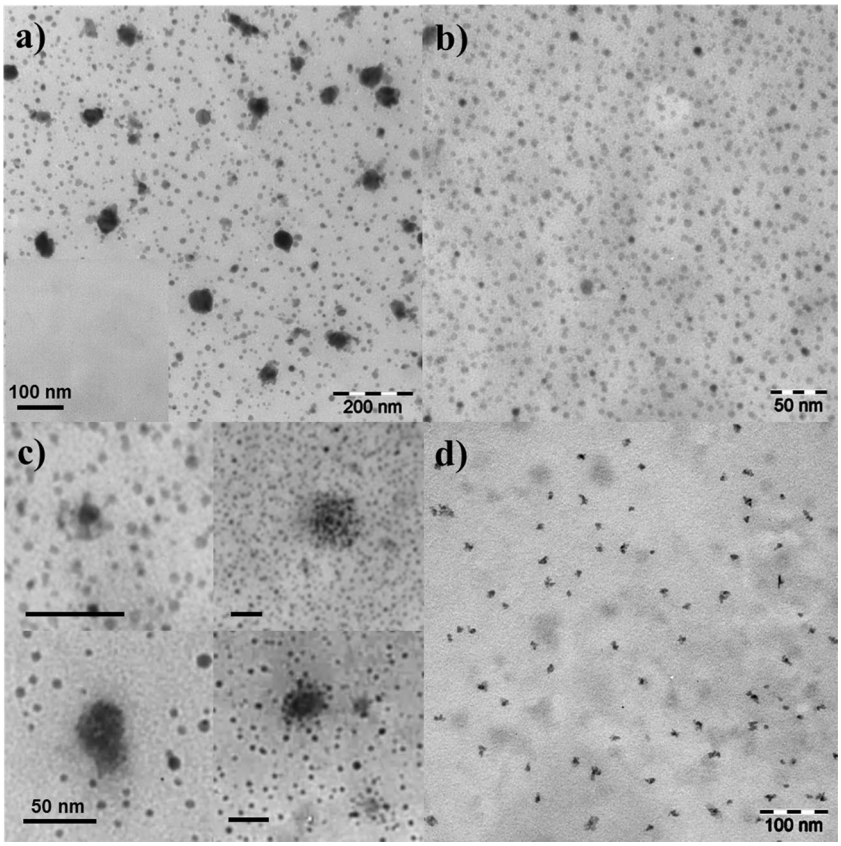

Fig. 3 TEM images of stained polymer particles of mPEG$_{114}$-*b*-p(Bz-*L*-Glu)$_{20}$-*b*-p(*L*-Leu)$_{10}$ at different magnifications after 20 (**a**,**b**,**c**) and 10 (**d**) min incubation with RuO_4. A TEM image of the deprotected copolymer is shown in the inset of (**a**)

the monomer feed ratios. The structure formation of these block copolymers in water was consistently analyzed by DLS and SANS. All block copolymers form in addition to micelles larger aggregates with radii in the range of 25 to 40 nm. The driving force for this process was analyzed by TEM and is summarized in Scheme 2. It should be noted that also nonequilibrium structures might be frozen in during the solvent evaporation when the samples are prepared for TEM analyses.

The block copolymers are formed from the water-soluble PEG block and two mutually immiscible blocks of p(Bz-*L*-Glu) and p(*L*-Leu) as well as p(Bz-*L*-Glu)-*co*-p(*L*-Leu), which form the core of the micelle. The block length of the p(Bz-*L*-Glu) block was kept at 20 repeat units, and the length of the p(*L*-Leu) was varied between 10 and 20 repeat units. It has been known from literature [57] that p(Bz-*L*-Glu) is a rigid polymer chain, which is able to form liquid crystalline structures. Both facts, the mutual immiscibility of the blocks and the self-assembly of p(Bz-*L*-Glu), led to the formation of a microphase separated micelle core. This in turn led to a non-uniform distribution of PEG blocks in the corona of the micelles, which seems to be a precondition for the formation of the large aggregates. Thus, the large aggregates can be described as clusters of micelles derived from hydrophobic interactions of the microphase separated micelle core.

Acknowledgments The authors would like to thank Dr. Donghui Zhang and her research group at LSU Baton Rouge for assistance with the GPC measurements. The authors also acknowledge the Oakridge Associated Universities program, which allowed for access to the Spallation Neutron Source, at Oakridge National Laboratory. JK thanks the Deutsche Forschungsgemeinschaft for financial support (FOR 1145).

References

1. Antonietti M, Förster S (2003) Vesicles and liposomes: a self-assembly principle beyond lipids. Adv Mater 15:1323–1333
2. Ahmed F, Pakunlu RI, Srinivas G, Brannan A, Bates F, Klein MI, Minko T, Discher DE (2006) Shrinkage of a rapidly growing tumor by drug-loaded polymersomes: pH-triggered release through copolymer degradation. Mol Pharm 3:340–350
3. Akagi T, Baba M, Akashi M (2007) Preparation nanoparticles by the self-organization of polymers consisting of hydrophobic and hydrophilic segments: potential applications. Polymer 48:6729–6747
4. Putnam D, Gentry CA, Pack DW, Langer R (2001) Polymer-based gene delivery with low cytotoxicity by a unique balance of side-chain termini. PNAS 98:1200–1205
5. Harada A, Kataoka K (2006) Supramolecular assemblies of block copolymers in aqueous media as nanocarriers relevant to biological applications. Prog Polym Sci 31:949–982
6. Blanazs A, Armes SP, Ryan AJ (2009) Self-assembled block copolymer aggregates: from micelles to vesicles and their biological applications. Macromol Rapid Commun 30:267–277
7. Loverde SM, Pantano DA, Christian DA, Mahmud A, Klein ML, Discher DE (2011) Curvature, rigidity, and pattern formation in functional polymer micelles and vesicles—from dynamic visualization to molecular simulation. Curr Opin Solid State Mater Sci 15:277–284
8. Rajagopal K, Mahmud A, Christian DA, Pajerowski JD, Brown AEX, Loverde SM, Discher DE (2010) Curvature-couples hydration of semicrystalline polymer amphiphiles yields flexible worm micelles but favors rigid vesicles: polycaprolactone-based block copolymers. Macromolecules 43:9736–9746
9. Israelachvili JN (1991) Intermolecular and surface forces, 2nd edn. Academic Press London, San Diego
10. Discher BM, Won Y-Y, Ege DS, Lee JC-M, Bates FS, Discher DE, Hammer DA (1999) Polymersomes: tough vesicles made from diblock copolymers. Science 284:1143–1146
11. Choucair A, Eisenberg A (2003) Control of amphiphilic block copolymer morphologies using solution conditions. Eur Phys J E 10:37–44
12. Kwon GS, Kataoka K (1995) Block copolymer micelles as long-circulating drug vehicles. Adv Drug Deliv Rev 16:295–309
13. Barz M, Duro Castano A, Vicent MJ (2013) A versatile post-polymerization modification method for polyglutamic acid: synthesis of orthogonal reactive polyglutamates and their use in click chemistry. Polym Chem 4:2989–2994
14. Lee HJ, Bae Y (2011) Cross-linked nanoassemblies from poly(ethylene glycol)-poly(aspartate) block copolymers as stable supramolecular templates for particulate drug delivery. Biomacromolecules 12:2686–2696
15. Giammona G, Cavallaro G, Pitarresi G, Pedone E (2000) Novel polyaminoacidic copolymers as nonviral gene vectors. Colloid Polym Sci 278:69–73
16. Byrne M, Thornton PD, Cryan SA, Heise A (2012) Star polypeptides by NCA polymerisation from dendritic initiators: synthesis and enzyme controlled payload release. Polym Chem 3:2825–2831
17. Rosu C, Selcuk S, Soto-Cantu E, Russo PS (2014) Progress in silica polypeptide composite colloidal hybrids: from silica cores to fuzzy shells. Colloid Polym Sci 292:1009–1040
18. Jeong SY, Moon HJ, Park MH, Joo MK, Jeong B (2012) Molecular captain: a light-sensitive linker molecule in poly(ethylene glycol)-poly(L-alanine-poly(ethylene glycol) triblock copolymer directs molecular nano-assembly, conformation and sol-gel transition. J Polym Sci 50:3184–3191
19. Song B, Song J, Zhang S, Anderson MA, Ao Y, Yang CY, Deming TJ, Sofroniew MV (2012) Sustained local delivery of bioactive nerve growth factor in the central nervous system via tunable diblock copolypeptide hydrogel depots. Biomaterials 33:9105–9116
20. Yang C-Y, Song B, Ao Y, Nowak AP, Abelowitz RB, Korsak RA, Havton LA, Deming TJ, Sofroniew MV (2009) Biocompatibility of amphiphilic diblock copolypeptide hydrogels in the central nervous system. Biomaterials 30:2881–2898
21. Hehir S, Cameron NR (2014) Recent advances in drug delivery systems based on polypeptides prepared from *N*-carboxyanhydrides. Polym Int 63:943–954
22. Ding J, Shi F, Xiao C, Lin L, Chen L, He C, Zhuang X, Chen X (2011) One-step preparation of reduction-responsive poly(ethylene glycol)-poly(amino acid)s nanogels as efficient intracellular drug delivery platforms. Polym Chem 2:2857
23. Breedveld V, Nowak AP, Sato J, Deming TJ, Pine DJ (2004) Rheology of block copolypeptide solutions: hydrogels with tunable properties. Macromolecules 37:3943–3953
24. Sgouras D, Duncan R (1990) Methods for the evaluation of biocompatibility of soluble synthetic polymers which have potential for biomedical use. 1. Use of the tretazolium based colorimetric assay (MTT) as a preliminary screen for evaluation of in vitro cytotoxicity. J Mater Sci 1:61–68
25. Harris, MJ (1992) Poly(ethylene glycol) chemistry, biotechnical and biomedical applications. In: Harris JM (ed) Topics in applied chemistry, Plenum Press, New York, pp 1–14

26. Abuchowski A, van Es T, Palczuk NC, Davis FF (1977) Alteration of immunological properties of bovine serum albumin by covalent attachment of polyethylene glycol. J Biol Chem 252:3578–3581
27. Abuchowski A, McCoy R, Palczuk NC, van Es T, Davis FF (1977) Effect of covalent attachment of polyethylene glycol on immunogenicity and circulating life of bovine liver catalase. J Biol Chem 252:3582–3586
28. Cabral H, Kataoka K (2014) Progress of drug-loaded polymeric micelles into clinical studies. J Control Release 190:465–476
29. Knop K, Hoogenboom R, Fisher D, Schubert US (2010) Poly(ethylene glycol) in drug delivery: pros and cons as well as potential alternatives. Angew Chem Int Ed 49:6288–6308
30. Greenwald RB (2001) PEG drugs: an overview. J Control Release 74:159–171
31. Gon S, Fang B, Santore MM (2011) Interaction of cationic proteins and polypeptides with biocompatible cationically-anchored PEG brushes. Macromolecules 44:8161–8168
32. Moghimi S, Hunter A, Murray J (2001) Long-circulating and target-specific nanoparticles: theory to practice. Pharmacol Rev 53:283–318
33. Obeid R, Armstrong T, Peng X, Busse K, Kressler J, Scholz C (2014) The behavior of poly(amino acids) containing *L*-cysteine and their block copolymers with poly(ethylene glycol) on gold surfaces. J Polym Sci A1(52):248–257
34. Obeid R, Scholz C (2011) Synthesis and self-assembly of well-defined Poly(amino acid) end capped Poly(ethylene glycol) and Poly(2-methyl-2-oxazoline). Biomacromolecules 12:3797–3804
35. Yokohama M, Kwon GS, Okano T, Sakurai Y, Sato T, Kataoka K (1992) Preparation of micelle-forming polymer-drug conjugates. Bioconjug Chem 3:295–301
36. Kataoka K, Kwon GS, Yokohama M, Okano T, Sakurai Y (1993) Block copolymer micelles as vehicles for drug delivery. J Control Release 24:119–132
37. Deng J, Gao N, Wang Y, Yi H, Fang S, Ma Y, Cai L (2012) Self-assembled cationic micelles based on PEG-PLL-PLLeu hybrid polypeptides as highly effective gene vectors. Biomacromolecules 13:3795–3804
38. Guenther M, Gerlach G, Wallmersperger T, Avula MN, Cho SH, Xie X, Devener BV, Solzbacher F, Tathireddy P, Magda JJ, Scholz C, Obeid R, Armstrong T (2013) Smart hydrogel-based biochemical microsensor array for medical diagnostics. Adv Sci Technol 85: 47–52
39. Armstrong T, Scholz C (2012) Investigation of the secondary structure of oligomeric poly(amino acid)s. Polym Prepr 53(1):600–601
40. Lee S, Spencer ND (2008) Adsorption properties of poly(L-lysine)-*graft*-poly(ethylene glycol) (PLL-*g*-PEG) at a hydrophobic interface: influence of tribological stress, pH, salt concentration, and polymer molecular weight. Langmuir 24:9479–9488
41. Scholz C (2007) Perspectives on: material aspects of retinal prostheses. J Bioact Compat Polym 22:539–568
42. Hell SW, Wichmann J (1994) Breaking the diffraction resolution limit by stimulated emission: stimulated-emission-depletion fluorescence microscopy. Opt Lett 19:780–782
43. Horkay F, Hammounda B (2008) Small angle neutron scatttering form typical synthetic and biopolymer solutions. Colloid Polym Sci 286:611–620
44. Daly WH, Poche D (1988) The preparation of N-carboxyanhydrides of α-amino acids using bis(trichloromethyl)carbonate. Tetrahedron Lett 29:5859–5862
45. Kricheldorf HR (2006) Polypeptides and 100 years of chemistry of a-amino acid N-carboxyanhydrides. Angew Chem Int Ed 45:5752–5784
46. Zou J, Fan J, He X, Zhang S, Wang H, Wooley KL (2013) A facile glovebox-free strategy to significantly accelerate the syntheses of well-defined polypeptides by N carboxyanhydride (NCA) ring-opening polymerizations. Macromolecules 46:4223–4226
47. Kricheldorf HR (1987) In: α-Amino acid-N-Carboxy-Anhydrides and related heterocycles, Springer, Berlin
48. Ulkoski D, Armstrong T, Scholz C (2013) Investigating the secondary structure of oligomeric poly(amino acid)s. In: Tailored polymer architectures for pharmaceutical and biomedical applications (ed.: C. Scholz, J. Kressler). ACS Symp Ser 1135:69–85
49. Ainavarapu SRK, Brujić J, Huang HH, Wiita AP, Lu H, Li L, Walther KA, Carrion-Vazquez M, Li H, Fernandez JM (2007) Contour length and refolding rate of a small protein controlled by engineered disulfide bonds. Biophys J 92:225–233
50. Lee H, Venable RM, MacKerell AD Jr, Pastor RW (2008) Molecular dynamics studies of polyethylene oxide and polyethylene glycol: hydrodynamic radius and shape anisotropy. Biophys J 95:1590–1599
51. Lee H, deVries A, Marrink SJ, Pastor RW (2009) A coarse-grained model for polyethylene oxide and polyethylene glycol: conformation and hydrodynamics. J Phys Chem B 113:13186–13194
52. Devanand K, Selser JC (1991) Asymptotic behavior and long-range interactions in aqueous solutions of poly(ethylene oxide). Macromolecules 24:5943–5947
53. Kyerematen SO, Busse K, Kohlbrecher J, Kressler J (2011) Synthesis and self-organization of poly(propylene oxide)-based amphiphilic and triphilic block copolymers. Macromolecules 44: 583–593
54. Gu PF, Xu H, Sui BW, Gou JX, Meng LK, Sun F, Wang XJ, Qi N, Zhang Y, He HB, Tang X (2012) Polymeric micelles based on poly(ethylene glycol) block poly(racemic amino acids) hybrid polypeptides: conformation-facilitated drug-loading behavior and potential application as effective anticancer drug carriers. Int J Nanomed 7:109–122
55. Trent JS (1984) Ruthenium tetraoxide staining of polymers: new preparative methods for electron microscopy. Macromolecules 17: 2930–2931
56. Letchford K, Burt H (2007) A review of the formation and classification of amphiphilic block copolymer nanoparticulate structures: micelles, nanospheres, nanocapsules and polymersomes. Eur J Pharm Biopharm 65:259–269
57. Asada T, Muramatsu H, Watanabe R, Onogi S (1980) Rheooptical studies of racemic poly(γ-benzyl glutamate) liquid crystals. Macromolecules 13:867–871